

## N O T I C E

THIS DOCUMENT HAS BEEN REPRODUCED FROM  
MICROFICHE. ALTHOUGH IT IS RECOGNIZED THAT  
CERTAIN PORTIONS ARE ILLEGIBLE, IT IS BEING RELEASED  
IN THE INTEREST OF MAKING AVAILABLE AS MUCH  
INFORMATION AS POSSIBLE

SQT

NASA CR 159826

BAT Report No. D2536-941005

(NASA-CR-159826) NASTRAN LEVEL 16 DEMONSTRATION MANUAL UPDATES FOR AEROELASTIC ANALYSIS OF BLADED DISCS (Textron Bell Aerospace Co., Buffalo, N. Y.) 15 p HC A02/MF A01	N81-19483  Unclas 18074
---	----------------------------------

CSCCL 20K G3/39

**NASTRAN LEVEL 16 DEMONSTRATION MANUAL UPDATES  
FOR AEROELASTIC ANALYSIS OF BLADED DISCS**

by

**V. ELCHURI  
A. M. GALLO**

**BELL AEROSPACE TEXTRON  
P. O. BOX 1  
Buffalo, New York 14240**

**NATIONAL AERONAUTICS AND SPACE ADMINISTRATION**

**CONTRACT NAS3-20382**

**NASA LEWIS RESEARCH CENTER  
CLEVELAND, OHIO**

**MARCH 1980**



NASA CR 159826

BAT Report No. D2536-941005

NASTRAN LEVEL 16 DEMONSTRATION MANUAL UPDATES  
FOR AEROELASTIC ANALYSIS OF BLADED DISCS

by

V. ELCHURI  
A. M. GALLO

BELL AEROSPACE TEXTRON  
P. O. BOX 1  
Buffalo, New York 14240

NATIONAL AERONAUTICS AND SPACE ADMINISTRATION

CONTRACT NAS3-20382

NASA LEWIS RESEARCH CENTER  
CLEVELAND, OHIO

MARCH 1980

## INTRODUCTION

A computer program based on state-of-the-art compressor and structural technologies applied to bladed shrouded discs has been developed and made operational in NASTRAN Level 16.

The problems encompassed include aéroelastic analyses, modes and flutter.

The program is documented in the form of five NASA Contractor's Reports — one Technical Report and four Updates to NASTRAN Level 16 Theoretical, User's, Programmer's and Demonstration manuals. This report describes the Demonstration manual updates.

DEMONSTRATION MANUAL UPDATES

RIGID FORMAT No. 16, Static Aerothermoelastic 'Design/Analysis'  
Aeroelastic 'Design/Analysis' of an Axial Flow Compressor Stage (16-1)

A. Description

This problem illustrates the use of the static aeroelastic analyses of the first stage rotor of an axial flow air compressor to determine,

i) the "as manufactured" blade shape required to produce the design point pressure ratio ("design" problem), and

ii) the operating point of the "flexible" designed blade ("analysis" problem). The total stiffness matrix, consisting of the elastic and geometric stiffness matrices, at any off-design operating point is saved for use in subsequent modal and flutter analyses. (See Demonstration Manual example 9-1).

The 43-blade rotor is designed to develop a total pressure ratio of 1.85 at a speed of 16043 rpm and an air flow rate of 73.15 lbm/sec. The finite element model of a representative sector of the rotor is shown in Figure 1.

B. Input

Bulk data cards used include DTI, STREAML1, PARAMETERS APRESS, ATEMP, FXCØØR, FYCØØR, FZCØØR, IPRTCF, IPRTCI, IPRTCL, KTØUT, PGEØM, SIGN, STREAML and ZØRIGN as illustrated in the User's Manual Section 1.15.3.

C. Analyses and Results

The rigid blade of Figure 1 produces a total pressure ratio of 1.85 at 16043 rpm and 73.15 lbm/sec air flow rate (Table 1). Because of the elasticity of the material, and under the action of centrifugal and aerodynamic pressure and thermal loads, the blade deforms and produces a total pressure ratio greater than the design value. A "redesign" of the rigid blade, considering the elastic and geometric properties of the bladed disc sector, enables determination of the "as manufactured" blade shape that, when loaded and deformed, would produce the design

pressure ratio. The 'rigid' performance of the "as manufactured" blade shape obtained at the end of the Design problem is also shown in Table 1.

This blade shape is then "Analyzed", in the current demonstration example, at the same (design) speed and flow rate to determine the 'flexible' operating pressure ratio. This value (1.84) can be further improved to approach the desired (1.85) pressure ratio by reducing the Parameters  $FXC\emptyset\emptyset R$ ,  $FYC\emptyset\emptyset R$  and  $FZC\emptyset\emptyset R$  in the Design problem (see User's Manual Section 1.15.3).

The blade shape at various stages during the Design and Analysis problems, as reflected by the grid point coordinates, is also shown in Tables 1 and 2. The coordinates are expressed in the basic system of Figure 1.

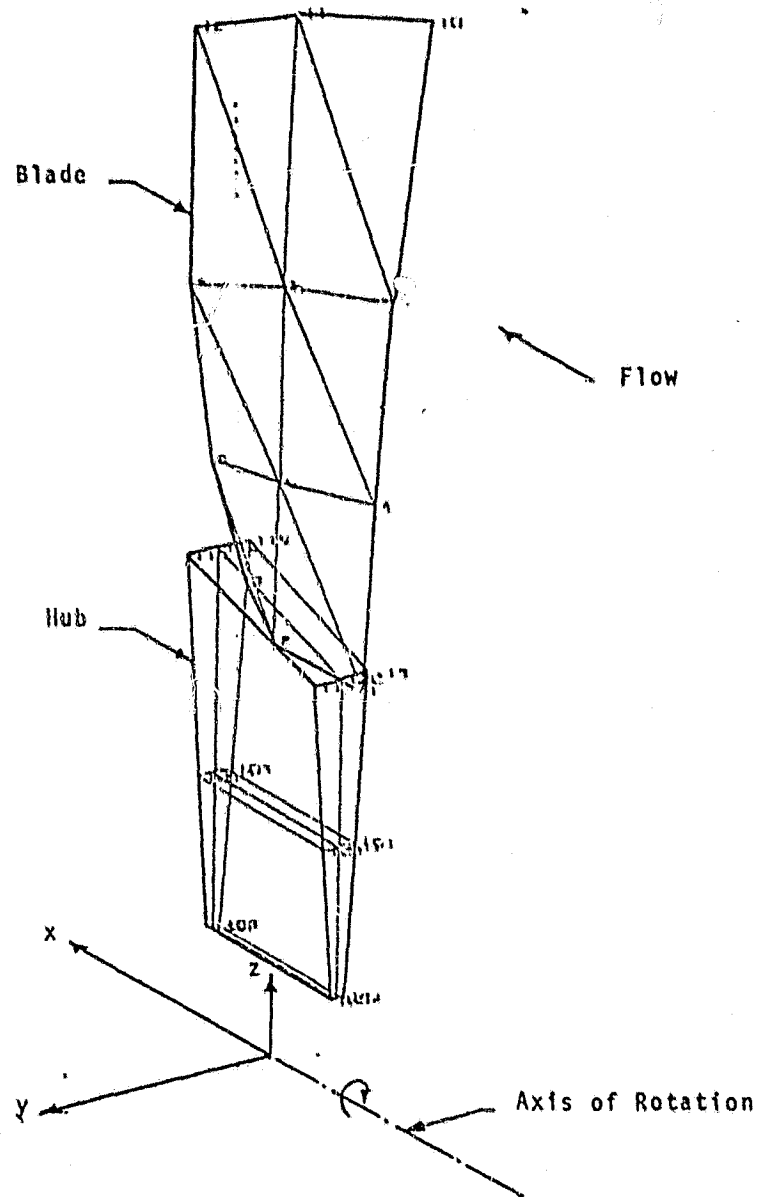


Figure 1. Finite Element Model of an Axial Flow Compressor Rotor Sector, and the Basic Coordinate System



Table 1. Design Problem

	Initial, Designed Blade 'Rigid' Performance			"As Manufactured" Blade 'Rigid' Performance		
Total Pressure Ratio	1.85			1.80		
Rotational Speed, rpm	16043			16043		
Air Flow Rate, lbm/sec	73.15			73.15		
Grid Points	X, in.	Y, in.	Z, in.	X, in.	Y, in.	Z, in.
1	-0.8980	-0.2732	3.7902	-0.8981	-0.2755	3.7796
2	0.0	0.0532	3.9996	-0.0001	0.0540	3.9986
3	0.8980	-0.2499	4.1926	0.8979	-0.2464	4.1847
4	-0.7630	-0.5004	5.4772	-0.7653	-0.4830	5.4554
5	0.0	0.0209	5.5000	-0.0005	0.0209	5.4985
6	0.7800	0.2342	5.4950	0.7799	0.2307	5.4889
7	-0.6290	-0.7494	7.3620	-0.6386	-0.7217	7.3281
8	0.0	0.0131	7.4000	-0.0091	0.0155	7.3976
9	0.6290	0.6369	7.3725	0.6240	0.6123	7.3416
10	-0.4240	-0.9330	9.9564	-0.4058	-1.1351	9.8905
11	0.0	-0.0221	10.0000	-0.0106	-0.0236	9.9970
12	0.4240	0.7598	9.9711	0.4140	0.8134	9.9304

Table 2. Analysis Problem

	"As Manufactured" Blade 'Rigid' Performance			"As Manufactured" Blade 'Flexible' Performance		
Total Pressure Ratio	1.80			1.84		
Rotational Speed, rpm	16043			16043		
Air Flow Rate, lbm/sec	73.15			73.15		
Grid Points	X, in.	Y, in.	Z, in.	X, in.	Y, in.	Z, in.
1	-0.8981	-0.2755	3.7796	-0.8979	-0.2814	3.7712
2	-0.0001	0.0540	3.9986	0.0001	0.0516	4.0003
3	0.8979	-0.2464	4.1947	0.8981	-0.2461	4.1795
4	-0.7653	-0.4830	5.4554	-0.7726	-0.4744	5.4413
5	-0.0005	0.0209	5.4985	-0.0031	0.0228	5.5033
6	0.7799	0.2307	5.4889	0.7797	0.2247	5.4889
7	-0.6386	-0.7217	7.3281	-0.6646	-0.7082	7.3062
8	-0.0091	0.0155	7.3976	-0.0157	0.0164	7.4058
9	0.6240	0.6123	7.3416	0.6303	0.5962	7.3237
10	-0.4058	-1.1351	9.8904	-0.5237	-1.1552	9.8520
11	-0.0106	-0.0236	9.9970	-0.0320	-0.0656	10.0079
12	0.4140	0.8134	9.9304	0.4130	0.7329	9.9093

RIGID FØRMAT No. 9 (APP AERØ), Aeroelastic Analysis

Modal, Flutter and Subcritical Roots Analyses of an Axial Flow  
Compressor Stage (9-5-1)

A. Description

The problem illustrates the use of the aeroelastic cyclic modal and flutter analyses of the first stage rotor of an axial flow air compressor to,

i) determine the natural frequencies and mode shapes of the bladed disc sector, of Figure 1, which exhibits rotational cyclic symmetry. The total stiffness matrix, including the differential stiffness effects at the operating point under consideration, saved during the Static Aerothermoelastic "Analysis" (see Demonstration Manual example 16-1) is used for the cyclic modal analysis.

ii) examine if the operating point being considered is a flutter point by analyzing the V-g and V-f plots based on user-selected combinations of densities, inter-blade phase angles and reduced frequencies, and in the process

iii) identify the subcritical (stable) roots.

B. Input

Bulk data cards used include AERØ, FLFACT, FLUTTER, MKAERØ1, STREAML1, STREAML2 and PARAMETERS IREF, KGGIN, LMØDES, MAXMACH, MINMACH, MTYPE and PRINT as described in the User's Manual Sections 1.15.2 and 1.15.5. Bulk data cards CYJØIN and PARAMETERS CTYPE, KINDEX and NSEGS are discussed in Section 1.12 of the User's Manual.

C. Analyses and Results

The finite element model of the bladed disc sector analyzed is shown in Figure 1. The first five zeroth harmonic natural frequencies and mode shapes of the sector are noted in Table 1. The grid points on the hub in contact with the compressor shaft were permitted radial translational degree of freedom only.

As a typical example, the first of the three frames of V-g and V-f plots output requested in this demonstration problem is shown in Figure 2. The density and interblade phase angle are held constant at  $(0.059 \times 1.507 \text{ E-6})$  slinch/in<sup>3</sup> and 180°, respectively, for this frame. The three reduced frequencies are identified by the symbols  $\ast(k=0.3)$ ,  $\circ(k=0.7)$  and  $\Delta(k=1.0)$ . The flutter summary for the three  $(\rho, \sigma, k)$  groups is presented in Table 2.

A close examination of the damping curves shows that the damping is nearly zero in the fourth mode of frequency 1797 Hz.

The implied density, velocity and reduced frequency are, respectively  $(0.059 \times 1.507 \text{ E-6})$  slinch/in<sup>3</sup>,  $1.055 \text{ E4}$  in/sec and 1.0 as compared with the actual values of these quantities as  $(0.059 \times 1.507 \text{ E-6})$  slinch/in<sup>3</sup>,  $1.910 \text{ E4}$  in/sec and 1.0, respectively.

The ratio  $V_{\text{implied}}/V_{\text{actual}}$  not being equal (or close) to 1.0 discounts the current operating point as being on a flutter boundary, at which all the three implied quantities must equal the actual quantities.

The demonstration example discussed has been presented principally for the purpose of illustrating the procedure for axial flow compressor flutter analysis. In order to locate the unstalled flutter boundaries over the entire region of operation of the compressor stage, similar analysis would be required for a series of operating points, harmonic numbers, interblade phase angles and reduced frequencies for both the stage rotor and the stator. Appropriate superposition of the rotor and stator results would then help identify the unstalled flutter boundaries on the compressor stage map.

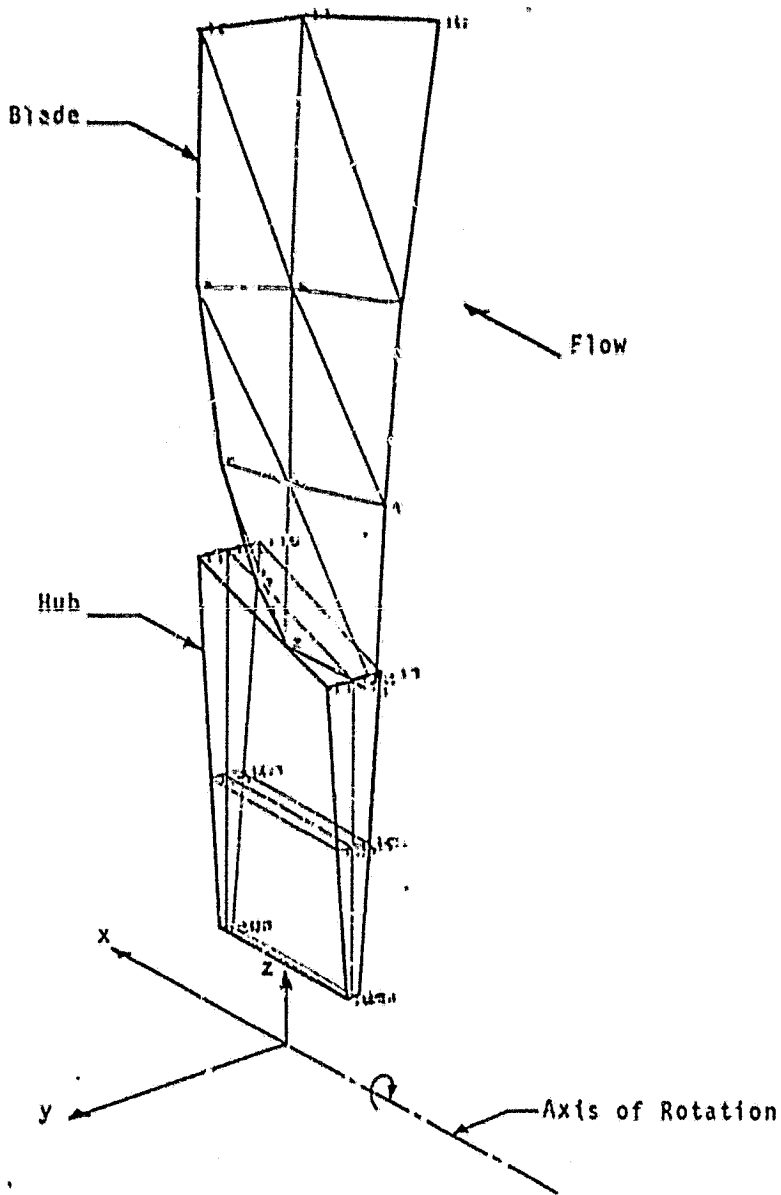


Figure 1. Finite Element Model of an Axial Flow Compressor Rotor Sector, and the Basic Coordinate System

Table 3. Bladed Disc Sector: Zeroth Harmonic Modes

Mode No.	1	2	3	4	5
Mode Frequency, Hz	471	790	977	1797	2154
Mode Shape	Circumferential Bending	Axial Bending	Torsion	Chordwise Bending (tip)	-



Table 2. Flutter Summary (k-Method)

$\rho\sigma k$ Group	Reduced Frequency k	Velocity V, in/sec	Damping g	Frequency f, Hz
$\rho_1\sigma_1k_1$	0.3	9.241 E3	-3.199 E-3	472
		1.549 E4	-2.291 E-3	791
		1.911 E4	-3.642 E-3	976
		3.530 E4	4.261 E-3	1803
$\rho_1\sigma_1k_2$	0.7	3.956 E3	-9.376 E-4	471
		6.633 E3	-6.666 E-4	790
		8.199 E3	-1.379 E-3	977
		1.508 E4	8.001 E-4	1798
$\rho_1\sigma_1k_3$	1.0	2.769 E3	-7.441 E-4	471
		4.643 E3	-6.892 E-4	790
		5.740 E3	-4.602 E-4	977
		1.055 E3	-8.848 E-5	1797